Neuron, Volume *95*

Supplemental Information

A C1-C2 Module in Munc13 Inhibits Calcium-Dependent Neurotransmitter Release

Francesco Michelassi, Haowen Liu, Zhitao Hu, and Jeremy S. Dittman

SUPPLEMENTAL FIGURES

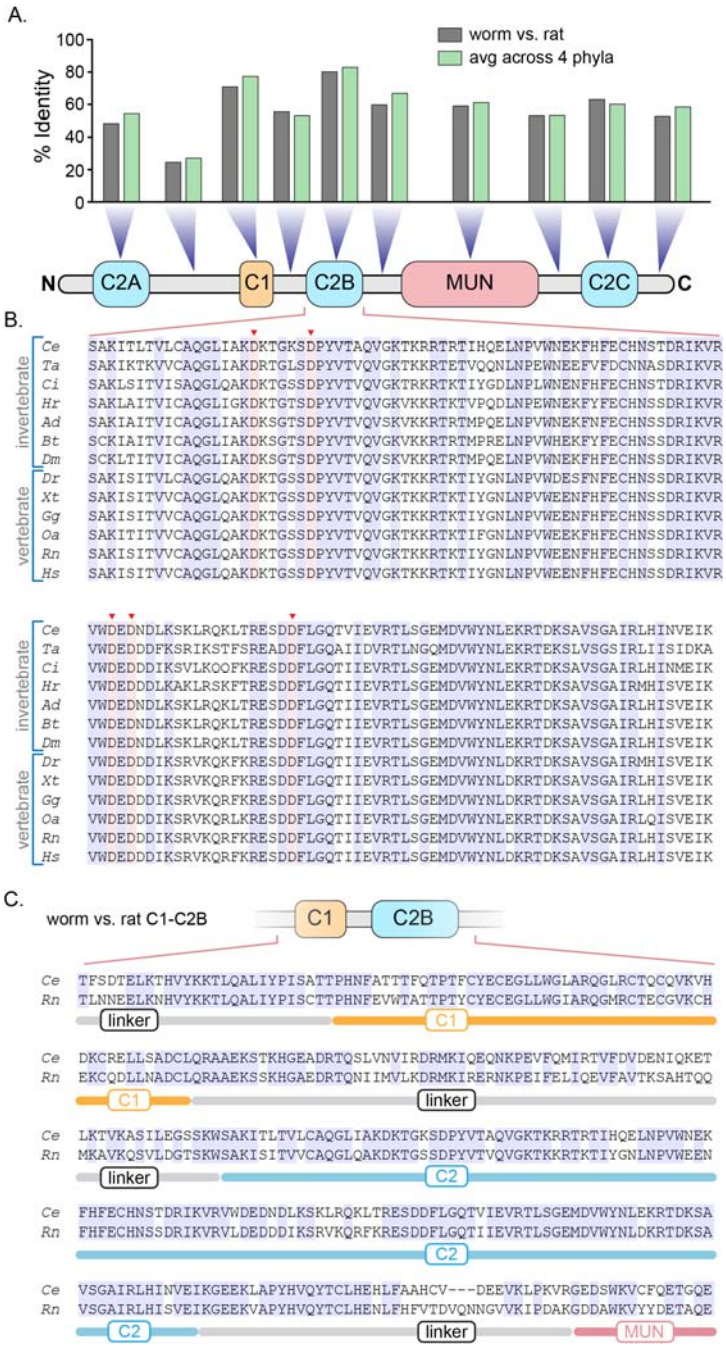

Figure S1. ***Related to Figure 1.*** **Primary sequence conservation of Munc13 across phylogeny.** **A.** Percent protein sequence identity for each region of Munc13 comparing rat Munc13-1 to *C. elegans* UNC-13L (*gray*) and an average percent identity for all six pair-wise comparisons for four representative species from four phyla/subphyla (*green*): vertebrates (rat), chordates (tunicate), arthropods (bumble bee), and nematodes (worm). **B.** C2B sequence alignment for several vertebrate and invertebrate UNC-13 homologs. Identical residues are highlighted (*blue*) and the five calcium-binding aspartates are indicated with arrowheads and highlighted in red. *Ce (Caenorhabditis elegans), Ta (Trichoplax adherens), Ci (Ciona intestinalis), Hr (Helobdella robusta), Ad (Anopheles darlingi), Bt (Bombus Terrestris), Dm (Drosophila melanogaster), Dr (Danio rerio), Xt (Xenopus tropicalis), Gg (Gallus gallus), Oa (Ornithorhynchus anatinus), Rn (Rattus norvegicus), Hs (Homo sapiens).* **C.** Protein sequence alignment for the C1-C2B tandem domain of rat Munc13-1 and *C. elegans* UNC-13 with identical residues highlighted in blue. This alignment shares 72% identity

and 81% similarity. For comparison, *C. elegans* and Trichoplax share about 53% identity and 73% similarity within the C1-C2B tandem domain.

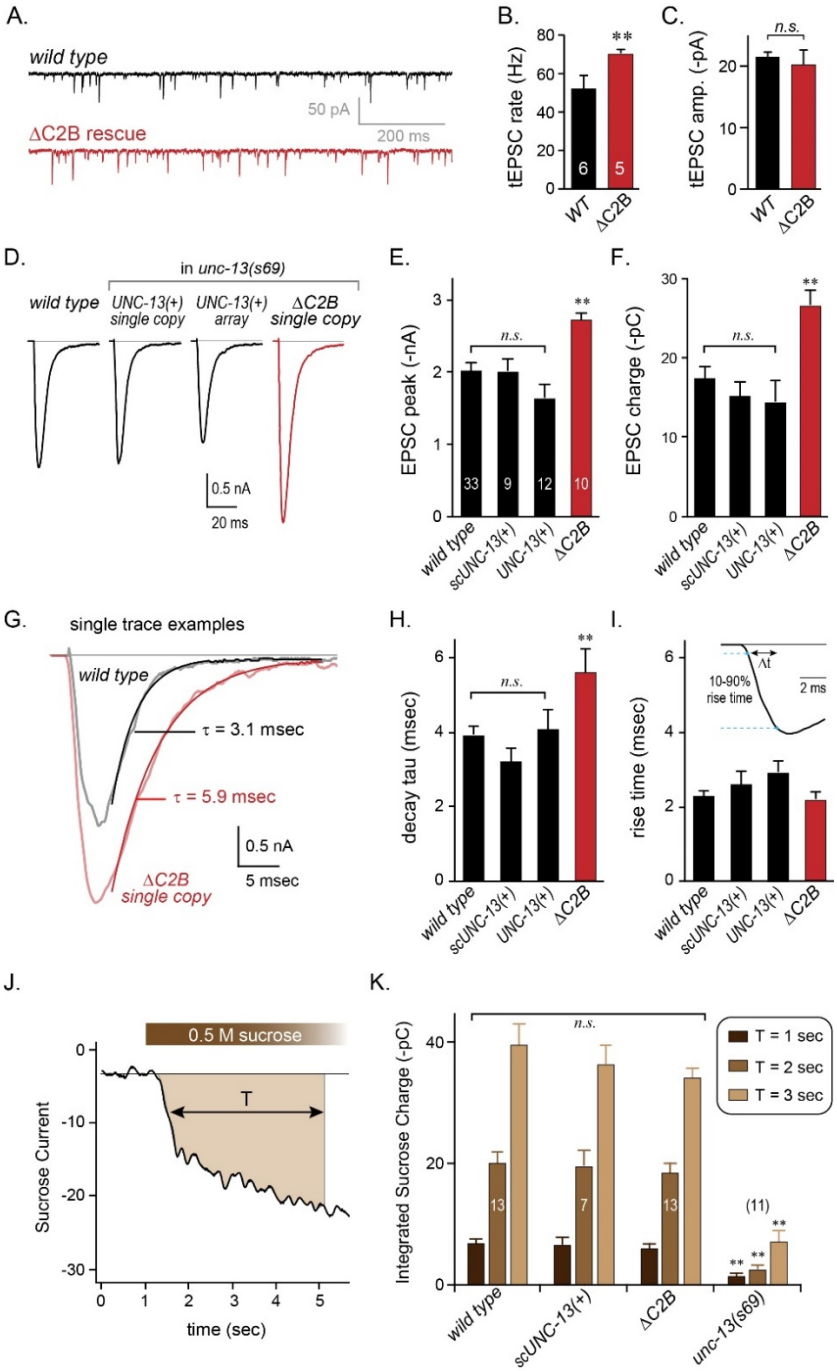

Figure S2. ***Related to Figure 1.*** **Comparison of wild-type and ΔC2B variants of UNC-13L.** **A.** Representative traces of tonic EPSCs (tEPSCs) for wild-type (*black*) and ΔC2B (*red*) transgenic animals in the unc-13 null mutant background. **B.** Average tEPSC rate (**B**) and amplitude (**C**). **D.** Average stimulus-evoked EPSCs for wild-type versus *unc-13(s69)* animals rescued with full-length single-copy UNC-13L (scUNC-13(+)) or a multi-copy extrachromosomal array of UNC-13L (UNC-13(+)) compared to rescue with UNC-13L(ΔC2B) (ΔC2B, *red*). Average EPSC peak (**E**) and cumulative charge (**F**) for the same strains. **G.** Representative examples of evoked EPSCs for wild-type (*black*) and DC2B (*red*) strains with single-exponential fits to characterize the current decay time. Average EPSC decay time constant (**H**) and 10-90% rise-time (**I**) for same strains. **J.** 500 mM sucrose triggers a large compound fusion event as the synaptic vesicle pool is rapidly mobilized and depleted. The total charge transfer due to vesicular release was estimated by integrating the current over time (T) and comparing across transgenic animals. **K.** Average sucrose-evoked charge transfer after 1, 2,

or 3 seconds is plotted for wild type, *unc-13(s69)*, and *unc-13(s69)* rescued with a single-copy transgene encoding either full-length UNC-13L (*scUNC-13(+)*) or ΔC2B. Errors bars are mean ± SEM, and experiment number given within the bars. ** $p < 0.01$, *n.s.* = not significant by ANOVA and Tukey-Kramer. *Strains*: *N2, unc-13(s69), JSD805, JSD1038, JSD1039*.

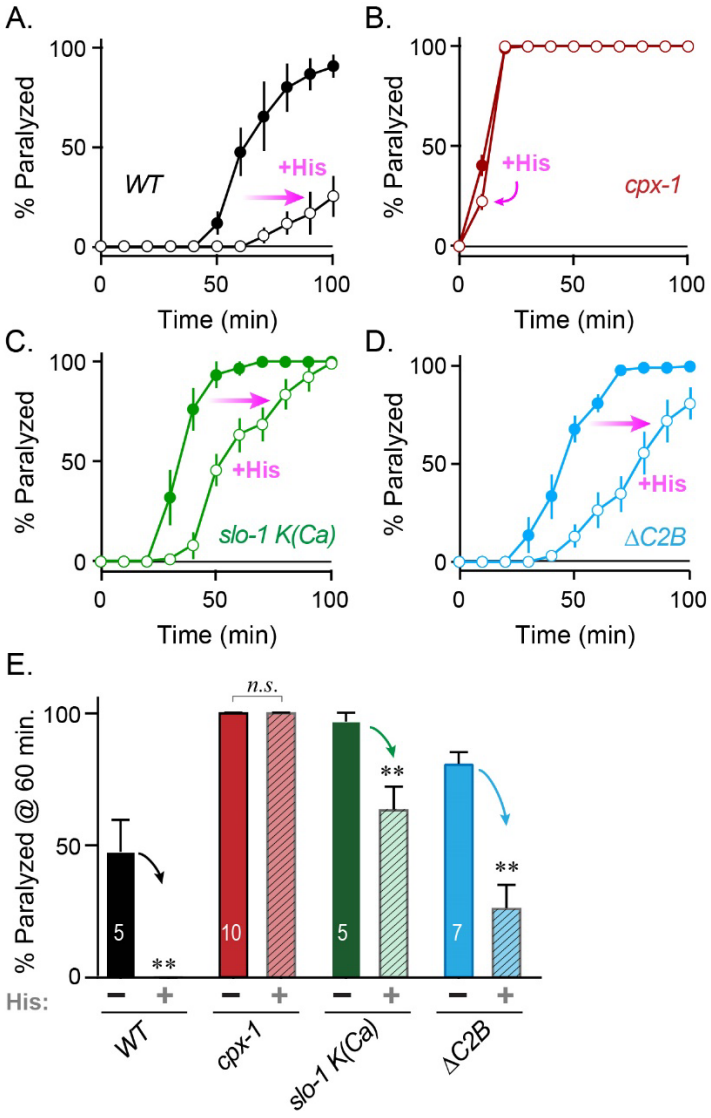

Figure S3. ***Related to Figure 1.*** **In vivo assay of enhanced calcium-dependent secretion. A – D.** Paralysis time course with (open circles) or without (closed circles) pretreatment with histamine for wild type (*black*), *cpx-1* mutants (*red*), *slo-1* K(Ca) mutants (*green*), and *unc-13(s69)* rescued with UNC-13L(ΔC2B) (*blue*). **E.** Average paralysis at 60 minutes for wild type (*black*), complexin *cpx-1(ok1552)* (*red*), BK channel *slo-1* (*green*), and ΔC2B rescue of *unc-13(s69)* (*blue*). All strains expressed the HisCl channel and were assayed either in the absence (*solid*) or presence (*hatched*) of 5 mM histamine. Errors bars are mean ± SEM (** $p < 0.01$, *n.s.* = not significant by ANOVA and Tukey-Kramer test for multiple comparisons). *Strains*: *JSD733, JSD758, JSD891, JSD895.*

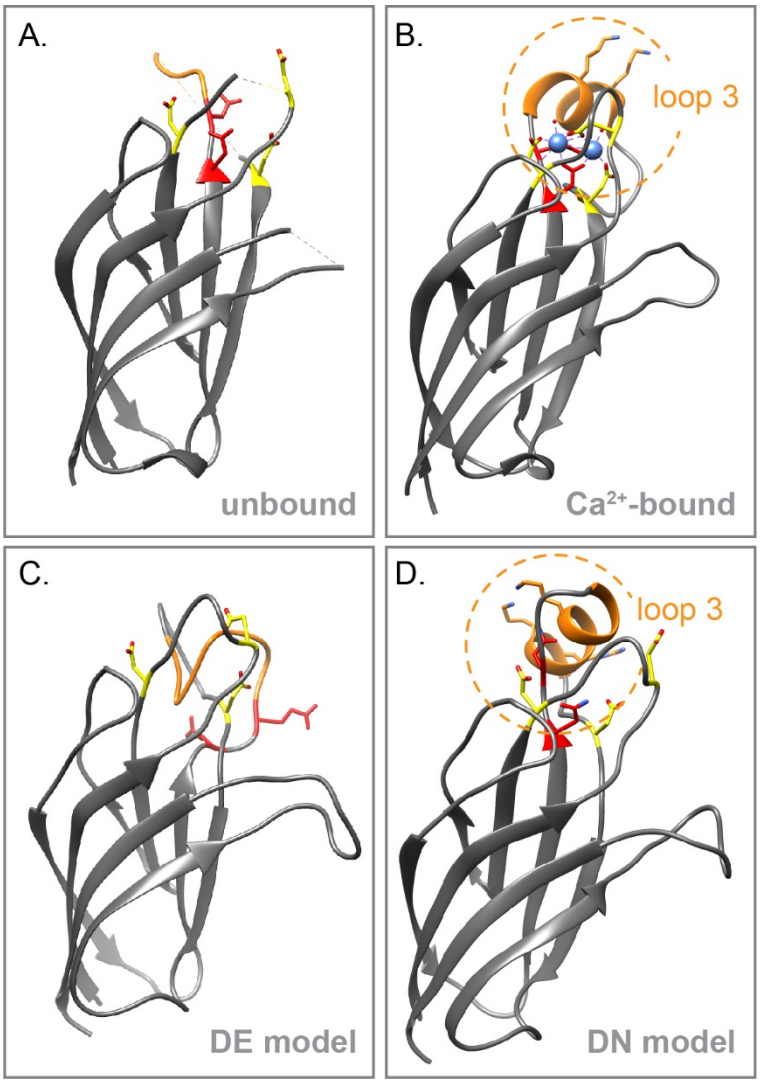

Figure S4. ***Related to Figure 2.*** **Comparing known and predicted Munc13-1 C2B domain structures. A.** Ribbon diagram of the crystal structure of Ca^{2+}-free C2B from Shin et al 2010. PDB: 3KWT. **B.** Ribbon diagram of the crystal structure of Ca^{2+}-bound C2B from Shin et al 2010. Calcium ions shown in blue. PDB: 3KWU. **C.** Predicted structure of C2B with D757E and D759E using Phyre2. **D.** Predicted structure of C2B with D757N and D759N using Phyre2. For all structures, loop 3 is highlighted in orange and the mutated loop 3 aspartates in red. The remaining aspartates are shown in yellow. Note the encircled alpha-helical loop 3 at the top of the C2B structures in panels **B** and **D** and the absence of this alpha helix in the other structures. We hypothesize that the formation of the loop 3 helix disrupts the C2B inhibitory interaction while promoting C2B insertion into the membrane.

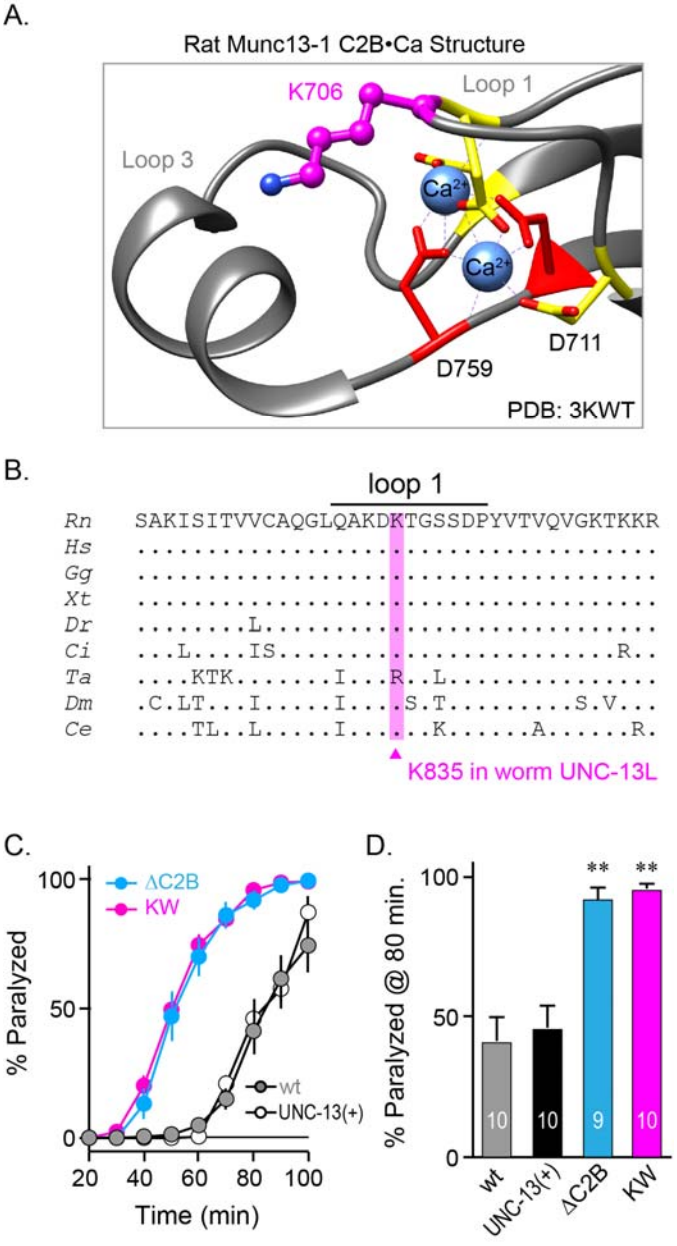

Figure S5. ***Related to Figure 3.*** **C2B Loop 1 KW substitution enhances secretion.** **A.** The calcium-binding pocket of rat Munc13-1 C2B (PDB 3KWT) from Shin et al 2010 with loop 1 lysine indicated in pink. **B.** Protein sequence alignment across several phyla (see **Figure 4** for details) centered on C2B loop 1 with the conserved lysine highlighted (*pink*). This residue corresponds to K706 in rat Munc13-1 and K835 in worm UNC-13. **C.** Average aldicarb time course for wild-type (*wt*, *gray*) or *unc-13(s69)* mutants rescued with full-length UNC-13 (UNC-13(+), *black*), ΔC2B (*blue*), or UNC-13 C2B K835W variant (KW, *pink*). **D.** Summary of aldicarb paralysis at 80 minutes for the same strains. Data are mean ± SEM and the number of independent assays is indicated on the bar graph for each genotype. Statistical comparisons were performed using ANOVA and Tukey-Kramer with genotypes differing from wild type designated by ** $p < 0.01$. *Strains*: *N2, JSD805, JSD830, JSD1038*.

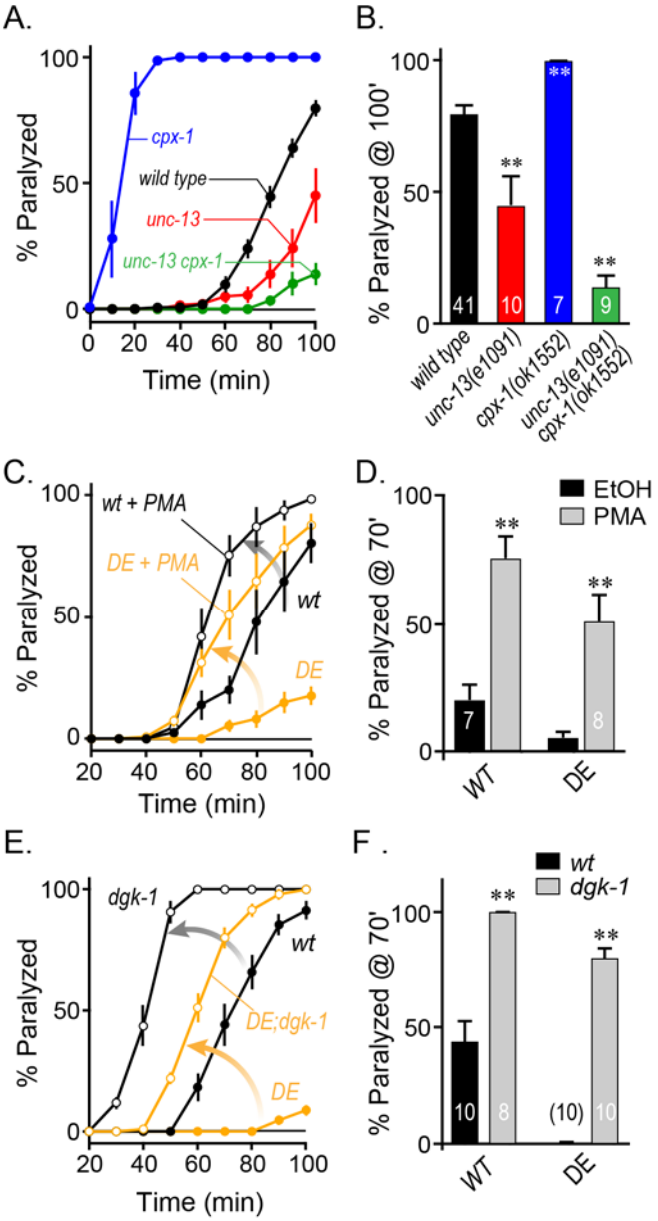

Figure S6. ***Related to Figure 5.*** **Aldicarb paralysis time courses for miscellaneous strains. A.** Average aldicarb time course for wild type (*black*), *unc-13(e1091)* (*red*), *cpx-1(ok1552)* (*blue*), and *unc-13 cpx-1* (*green*). **B.** Paralysis at 100 minutes in 1 mM aldicarb for these same genotypes. **C.** Average aldicarb time course for wild-type or *unc-13(s69)* mutants rescued with the UNC-13 C2B DE variant (DE) following exposure to phorbol ester. Strains were assayed following pretreatment with either phorbol 12-myristate 13-acetate (PMA, *orange*) or vehicle control (*black*). **D.** Summary of aldicarb paralysis at 70 minutes for wild-type and DE rescue strains following pretreatment with either ethanol vehicle (EtOH, *black*) or 0.25 μg/mL PMA (PMA, *gray*). **E.** Average aldicarb time course for wild type (*black, filled circles*), *dgk-1(nu62)* (*black, open circles*), DE (*orange, filled circles*), and DE;*dgk-1* (*orange, open circles*). **F.** Aldicarb paralysis at 70 minutes is plotted for wild type UNC-13 (WT) and DE in either a wild-type (*black*) or *dgk-1* DAGK mutant background (*gray*). Data are mean ± SEM and the number of independent assays is indicated on the bar graph for each genotype. Statistical comparisons were performed using ANOVA and Tukey-Kramer with genotypes differing from wild type designated by ** $p < 0.01$, *n.s.* = not significant.